



Usnic acid as calcium ionophore and mast cells stimulator

Maria A. Chelombitko¹, Alexander M. Firsov¹, Elena A. Kotova, Tatyana I. Rokitskaya, Ljudmila S. Khailova, Lyudmila B. Popova, Boris V. Chernyak, Yuri N. Antonenko*

Belozersky Institute of Physico-Chemical Biology, Lomonosov Moscow State University, 119991 Moscow, Russia

ARTICLE INFO

Keywords:

Usnic acid
Mast cells
Mitochondrial uncoupler
Protonophore
Membrane potential
Calcium ionophore

ABSTRACT

Usnic acid (UA), a secondary lichen metabolite, has long been popular as one of natural fat-burning dietary supplements. Similar to 2,4-dinitrophenol, the weight-loss effect of UA is assumed to be associated with its protonophoric uncoupling activity. Recently, we have shown that the ability of UA to shuttle protons across both mitochondrial and artificial membranes is strongly modulated by the presence of calcium ions in the medium. Here, by using fluorescent probes, we studied the calcium-transporting capacity of usnic acid in a variety of membrane systems comprising liposomes, isolated rat liver mitochondria, erythrocytes and rat basophilic leukemia cell culture (RBL-2H3). At concentrations of tens of micromoles, UA appeared to be able to carry calcium ions across membranes in all the systems studied. Similar to the calcium ionophore A23187, UA caused degranulation of RBL-2H3 cells. Therefore, UA, being a protonophoric uncoupler of oxidative phosphorylation, at higher concentrations manifests itself as a calcium ionophore, which could be relevant to its overdose toxicity in humans and also its phytotoxicity.

1. Introduction

Usnic acid (UA), a natural dibenzofuran derivative, abundantly produced by lichens, is known to exhibit a variety of therapeutic activities, e.g., antibacterial, antiviral, anti-inflammatory, antioxidant and antitumor activities [1,2]. The fat-burning activity, along with several beneficial medicinal properties of UA is supposed to be associated with the ability of this compound to facilitate proton cycling across membranes, similar to conventional uncouplers, such as DNP and CCCP. According to our recent study [3], the protonophoric activity of UA is significantly stimulated by calcium ions, apparently due to calcium-assisted formation of UA dimers, which are responsible for transmembrane proton cycling. Therefore, it could be suggested that UA is also able to carry Ca^{2+} across artificial and natural membranes. This issue is of high importance, because any disturbance of calcium homeostasis linked to regulation of key cell functions is assumed to be toxic.

An example of such a process is influx of calcium into mast cells induced by calcium ionophores such as A23187 [4–6], ionomycin [7] and omomycin [8,9], which have long been known to stimulate mast cell secretion, i.e. release of pre-formed mediators such as histamine [10] from their granules, the process called degranulation [11]. Here,

we used the rat basophilic leukemia cell line (RBL-2H3), a histamine-releasing mast cell analogue, commonly utilized for in vitro studies of degranulation [12–14], as a test system to examine the ability of UA to transport calcium ions into cells. By monitoring release of the enzyme β -hexosaminidase from secretory granules [15], we showed that UA caused RBL-2H3 cells degranulation. Simultaneously, we observed Ca^{2+} entry into the cells by using the calcium-sensitive probe Fluo-3-AM.

In addition, we report data on the ability of UA to carry calcium ions across liposomal, mitochondrial and erythrocyte membranes, thereby showing that UA can exhibit properties of a calcium ionophore.

2. Materials and methods

2.1. Materials

Most chemicals including (R)-(+)-usnic acid (UA) were from Sigma (USA). BAPTA-AM, Fluo-4-AM, Fluo-3-AM, Fluo-5 N, and Magnesium Green AM were from Molecular probes (USA).

Abbreviations: UA, usnic acid; RR, Ruthenium Red; DNP, 2,4-dinitrophenol; CCCP, carbonyl cyanide *m*-chlorophenylhydrazine; RBL-2H3, rat basophilic leukemia cell culture; BAPTA-AM, 1,2-bis (2-aminophenoxy) ethane-*N,N,N',N'*-tetraacetic acid acetoxymethyl ester

* Corresponding author.

E-mail address: antonen@genebee.msu.su (Y.N. Antonenko).

¹ Contributed equally to this work.

<https://doi.org/10.1016/j.bbamem.2020.183303>

Received 3 February 2020; Received in revised form 14 March 2020; Accepted 31 March 2020

Available online 03 April 2020

0005-2736/ © 2020 Elsevier B.V. All rights reserved.

2.2. Efflux of calcium and zinc from liposomes

Ca^{2+} - (Zn^{2+})-loaded liposomes were prepared by evaporation under a stream of nitrogen of a 2% solution of diphyanoylphosphatidylcholine (DPhPC, Avanti Polar Lipids) lipid (5 mg) in chloroform followed by hydration with 0.5 ml of a buffer solution containing 100 mM CaCl_2 (100 mM ZnCl_2), 30 mM MES, 30 mM Tris, pH = 7.4. The mixture was vortexed, passed through several cycles of freezing and thawing, and extruded through 0.1- μm pore size Nucleopore polycarbonate membranes using an Avanti Mini-Extruder. The unbound calcium or zinc was then removed by passage through a Sephadex G-50 coarse column with a buffer solution containing 180 mM sucrose 10 mM KCl, pH = 7.4. Fluorescence of Fluo-5n was monitored at 520 nm (excitation at 495 nm) with a Panorama Fluorat O2 spectrofluorimeter (Lumex, Russia).

2.3. Calcium transport in isolated rat liver mitochondria

Rat liver mitochondria were isolated from male rats by differential centrifugation [16] in a medium containing 250 mM sucrose, 5 mM MOPS, 1 mM EGTA, pH 7.4. The final washing was performed in the medium additionally containing bovine serum albumin (0.1 mg/ml). Protein concentration was determined using the Biuret method. Handling of animals and experimental procedures were conducted in accordance with the international guidelines for animal care and use and were approved by the Institutional Ethics Committee of A.N. Belozersky Institute of Physico-Chemical Biology at the Moscow State University.

2.4. Measurement of calcium ions efflux from isolated mitochondria

Extramitochondrial Ca^{2+} changes were measured with Fluo-5 N, a low-affinity Ca^{2+} indicator, as described previously [17]. Isolated rat liver mitochondria (protein 0.5 mg/ml) were resuspended in 250 mM sucrose, 10 mM Tris, 10 mM KH_2PO_4 , pH 7.4, 1 mM succinate, 2 μM rotenone, 1 μM cyclosporine A with 1 μM Fluo-5 N. Fluorescence changes (excitation 495 nm, emission 515 nm) were recorded at room temperature using the Panorama Fluorat O2 spectrofluorimeter.

2.5. Measurement of calcium and magnesium ions influx into erythrocytes

Blood samples from a healthy donor were collected on the day of each experiment in phosphate-buffered saline (PBS, 150 mM NaCl, 10 mM KH_2PO_4 , pH 7.4) containing EDTA (1 mM), and the erythrocytes were then washed twice in PBS without EDTA, as described previously [18]. The resulting erythrocytes were re-suspended in HEPES buffer (125 mM NaCl, 3 mM KCl, 1 mM MgCl_2 , 2 mM CaCl_2 , 16 mM HEPES, 1.2 mM sodium phosphate, and 10 mM glucose, pH 7.4) so that hematocrit values would reach 5%. Fluo-4-AM was loaded into erythrocytes as described in [19] via incubation of the dye (1 μg) during 30 min in HEPES buffer at $T = 37^\circ\text{C}$ and hematocrit 1%. Erythrocytes were washed three times in HEPES buffer to remove the unloaded dye. Fluorescence changes (excitation 495 nm, emission 515 nm) were recorded at room temperature using the Panorama Fluorat O2 spectrofluorimeter.

To measure the transport of magnesium ions, the dye Magnesium Green AM (MagGreen-AM) was loaded into erythrocytes via incubation of the dye (20 μM) during 30 min in HEPES buffer at $T = 37^\circ\text{C}$ and hematocrit 1% in the presence of 0.02% pluronic F127 to increase the dye loading. Erythrocytes were washed three times in HEPES buffer to remove the unloaded dye.

2.6. Culture of RBL-2H3 cells

RBL-2H3 cells were cultivated in the medium containing 70% α -MEM, 20% RPMI-1640, 10% heat-inactivated fetal bovine serum (HI-

FBS), 2 mM L-glutamine (PanEko, Russia) at 37°C и 5% CO_2 . The cells were passaged every 3 days at 1:4 to 1:8 dilution.

2.7. Fluorescence microscopy

Cells were plated on 35-mm² confocal dishes (100,000 cell/ml). The next day, cells were stained with Fluo-3-AM (Invitrogen) and LysoTracker Red DND-99 (Invitrogen) to visualize the level of intracellular calcium and mast cell secretory granules, respectively. Cells were incubated with 5 μM Fluo-3-AM and 2.5 mM probenecid for 30 min at 37°C and 5% CO_2 . After washing the cells with HBSS, LysoTracker Red DND-99 was added at a concentration of 100 nM and incubated for 30 min at 37°C and 5% CO_2 . Along with lysosomes, LysoTracker identifies secretory granules because their pH is 5.5 [20]. After washing in the HBSS, cells were stained with 2 $\mu\text{g}/\text{ml}$ Hoechst 33342 and observed using an Axiovert 200 M fluorescence microscope (Carl Zeiss) equipped with an AxioCAM HRM camera at a magnification of $\times 1000$.

2.8. β -Hexosaminidase assay

RBL-2H3 cells were plated on 24-well plates at a concentration of 100,000 cells/ml. The next day, the medium was replaced with Hank's Balanced Salt Solution (HBSS) (PanEco, Russia) and UA was added at final concentrations of 0.2, 1, 4, 7 and 10 μM . The cells were incubated for 30 min at 37°C and 5% CO_2 . The calcium ionophore A23187 (1 μM) was used as a well-known activator of mast cells degranulation. To evaluate the level of spontaneous degranulation, DMSO at a concentration of 0.1% was added to control wells. To assess the contribution of intracellular calcium to cell responses to UA and the calcium ionophore A23187, cells were pretreated with the intracellular calcium chelator BAPTA-AM (20 μM) for 30 min before stimulation of degranulation. The enzyme β -hexosaminidase, located in secretory granules [15], was used as a marker of RBL-2H3 cells degranulation. The amount of this enzyme in the conditioned medium and the cell lysate was determined by the release of methylumbelliferone from 4-methylumbelliferyl-N-acetyl- β -D-glucosaminide according to the standard method [20]. After activation of degranulation, the culture medium was aspirated. The cells were lysed with an equal volume of 0.2% Triton X-100 in HBSS and incubated for 10 min at 37°C . The conditioned medium was centrifuged for 7 min at 4390 g at 4°C . The supernatant was assayed for β -hexosaminidase activity. For this, 25 μl of samples was added in the wells of a 96-well black plate to 100 μl of a 1.8 mM solution of 4-methylumbelliferyl-N-acetyl- β -D-glucosaminide (substrate for β -hexosaminidase) in 40 mM citrate buffer (pH 4.5). The mixture was incubated for 30 min at 37°C . The reaction was stopped by adding 175 μl of 200 mM glycine/NaOH buffer (pH 10.7). Fluorescence was measured with a Thermo Fluoroscan Ascent spectrofluorimeter at 460 nm (excitation wavelength 355 nm). The release level of β -hexosaminidase (%) in the sample was determined using the formula $A/(A + B) \times 100\%$, where A is fluorescence intensity of the conditioned medium, and B is fluorescence intensity of the cell lysate.

3. Results and discussion

3.1. Ca^{2+} efflux from liposomes

To study transport of calcium ions across model lipid membranes, we prepared calcium-loaded liposomes and monitored calcium efflux by using the calcium-sensitive fluorescent dye Fluo-5 N. The addition of UA at micromolar concentrations caused calcium efflux from the liposomes similar to ionomycin, which was added at the end of each recording as a positive control (Fig. 1A). The dye Fluo-5 N also appeared to be responsive to zinc ions, as the addition of ionomycin, known to effectively transport Zn^{2+} [21], induced fast zinc efflux from Zn^{2+} -loaded liposomes (Fig. 1B). By contrast, UA did not induce Zn^{2+} efflux

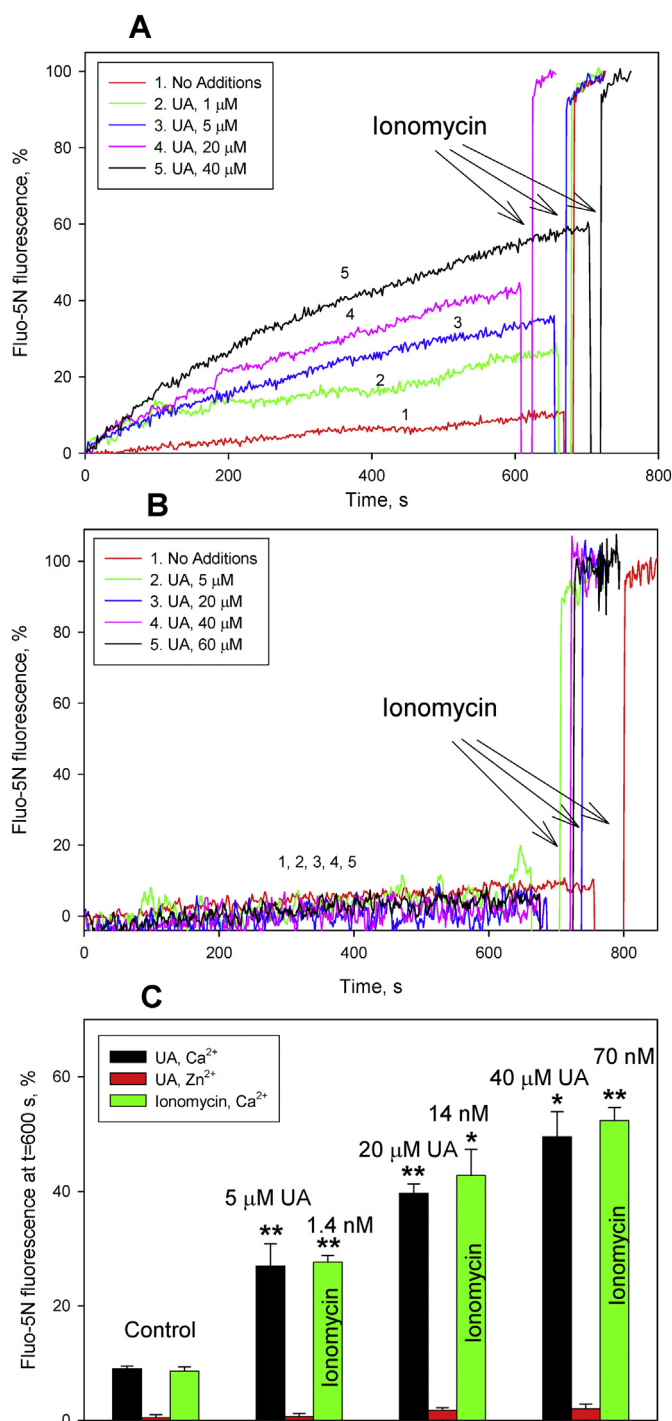


Fig. 1. Kinetics of calcium (A) or zinc (B) efflux from liposomes as a function of the concentration of usnic acid (added at time zero) measured by fluorescence of the calcium-sensitive dye Fluo-5 N (1 μ M). C. Percent of calcium (black and green bars) or zinc (red bars) efflux from liposomes at $t = 600$ s induced by various concentrations of UA (black bars) and ionomycin (green bars). Results are expressed as mean \pm SEM ($n = 3$), * $p < .05$; ** $p < .01$, Student's t -test. Liposomes made from DPhPC lipid were loaded with 100 mM CaCl₂ or ZnCl₂. The solution was 180 mM sucrose, 10 mM Tris, 10 mM MES, 10 mM KCl, pH = 7.4. Lipid concentration was 10 μ g/ml. Ionomycin (0.7 μ M) was added after approximately 10 min showing 100% of the cations efflux. (For interpretation of the references to colour in this figure legend, the reader is referred to the web version of this article.)

from the liposomes even at tens of micromoles. These data unambiguously show that UA-induced Ca²⁺ efflux from liposomes is not a consequence of a nonspecific increase in permeability of liposomal membranes, but results from UA functioning at high concentrations as a selective calcium ionophore, with the ion selectivity differing from that of A23187 and that of ionomycin [21]. The acting concentrations of UA were higher than those for ionomycin by about three orders of magnitude, as follows from dose dependences shown in Fig. 1C. Taking into account some structural correspondence between UA and the other known calcium ionophore ferutinin, the mechanistic similarity between calcium transport mediated by UA and ferutinin, in particular, formation of a complex of Ca²⁺ with two ionophore molecules as an important step in the transport process [22,23], could be suggested. Of note, the ability to carry Ca²⁺ was also supported by our previous data on the UA-mediated Ca²⁺ extraction to hydrophobic phase [3].

It is well known that carrier-mediated calcium transport across membranes either can be accompanied by transmembrane movement of electrical charges (e.g. electrogenic transport observed for ferutinin [23]) or can be electrically silent owing to back transfer of protons (as in the case of ionomycin or A23187). To ascertain the type of transport mediated by UA, we tested the effect of valinomycin on the calcium efflux from liposomes. Valinomycin is known to increase the rate of electrogenic transport but not that of electroneutral transport. As shown in Fig. 2 (blue and pink curves), valinomycin was effective in the case of UA, thereby suggesting the electrogenic nature of the UA-mediated calcium transport. By contrast, no effect of valinomycin was observed in the case of the ionomycin-mediated calcium transport (gray and black curves).

3.2. Ca²⁺ efflux from isolated mitochondria

According to our earlier paper [3], usnic acid induced efflux of calcium ions from isolated mitochondria, as detected by using Fluo-5 N. This Ca²⁺ efflux observed at low UA concentrations (of the order of 1 μ M) is similar to that found previously with other mitochondrial protonophoric uncouplers such as CCCP [24–26]. The mechanism of the uncoupler-induced Ca²⁺ efflux was associated with reversal of Ca²⁺ entry via the mitochondrial calcium uniporter MCU as a result of membrane potential collapse. Consistently, the uncoupler-induced Ca²⁺ efflux was abolished by the specific MCU inhibitor Ruthenium Red (RR). Here, we found that at high concentrations (starting from 10 μ M) UA is able to induce Ca²⁺ efflux even in the presence of RR (Fig. 3). The subsequent addition of A23187 led to only small increase of the efflux.

3.3. Ca²⁺ influx into erythrocytes

We also studied the ability of UA to carry calcium ions across the plasma membrane by monitoring Ca²⁺ influx into human erythrocytes. The addition of UA at a concentration of 10 μ M resulted in almost complete Ca²⁺ entry into erythrocytes (Fig. 4, green curve), as only a small increase in the fluorescence of the calcium-sensitive probe was observed upon the subsequent addition of ionomycin. By contrast, UA at the same concentration was unable to transport magnesium ions into erythrocytes, as measured by the fluorescence of the Mg²⁺ – sensitive probe MagGreen (Fig. 4, blue curve). In the case of Mg²⁺ transport, the addition of ionomycin after UA brought about a large increase in the fluorescence signal. Thus, in erythrocytes UA also manifested itself as a selective calcium ionophore.

3.4. Fluorescence imaging of intracellular Ca²⁺ and granule dynamics in RBL-2H3 cells

In further experiments, by using immunofluorescence microscopy, we explored the impact of UA in comparison with that of A23187 on the intracellular Ca²⁺ level and secretory granule dynamics in RBL-2H3

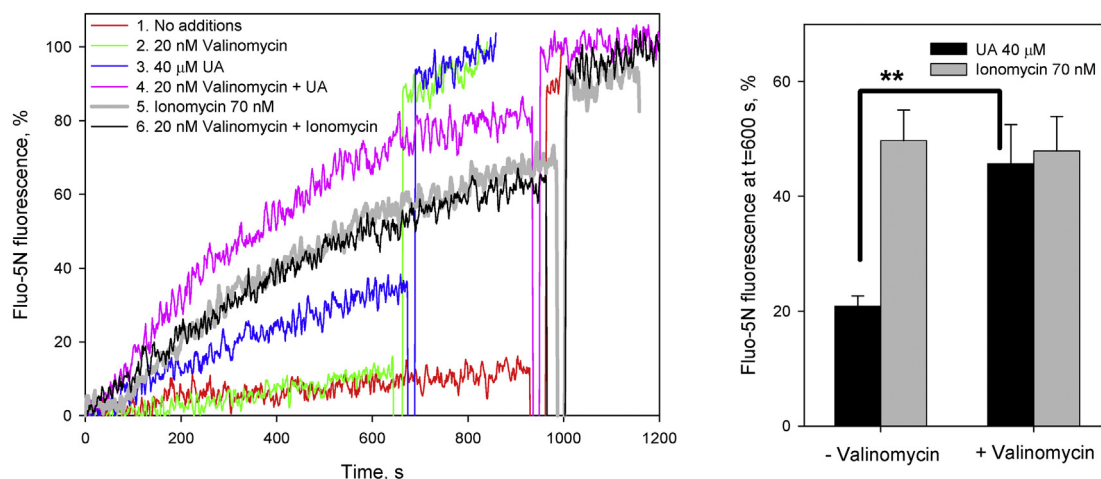


Fig. 2. A. Effect of the potassium ionophore valinomycin (20 nM) on the kinetics of calcium efflux from liposomes mediated by usnic acid (added at time zero, 40 μ M, blue and pink curves) or by ionomycin (70 nM, gray and black curves), as measured by fluorescence of the calcium-sensitive dye Fluo-5 N (1 μ M). B. Percent of calcium efflux from liposomes at t = 600 s mediated by UA (filled bars) or ionomycin (gray bars) without valinomycin (left) and in the presence of valinomycin (right). Results are expressed as mean \pm SEM (n = 3), ** p < 0.01, Student's t-test. (For interpretation of the references to colour in this figure legend, the reader is referred to the web version of this article.)

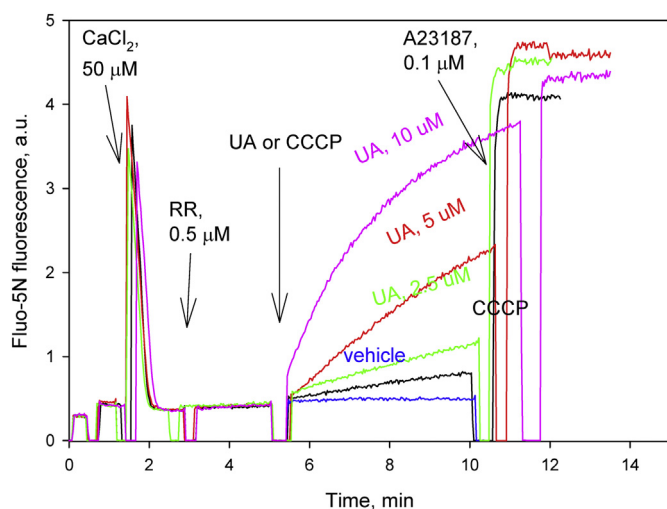


Fig. 3. Effect of UA (green curve, 2.5 μ M; red curve, 5 μ M; pink curve, 10 μ M) and the calcium ionophore A23187 (0.1 μ M) on the efflux of calcium ions from Ca²⁺-preloaded mitochondria with subsequent addition of Ruthenium Red (RR, 0.5 μ M). Extramitochondrial Ca²⁺ was measured by Fluo-5 N fluorescence (1 μ M). Incubation mixture: 250 mM sucrose, 10 mM Tris, 10 mM KH₂PO₄, pH 7.4, 1 mM succinate, 2 μ M rotenone, 1 μ M cyclosporin A. Mitochondrial protein, 0.5 mg/ml. Black curve shows the effect of 200 nM CCCP. (For interpretation of the references to colour in this figure legend, the reader is referred to the web version of this article.)

cells (Fig. 5). Intracellular calcium detected with the Ca²⁺ indicator dye Fluo-3-AM was seen mainly as weakly visible individual clusters in the cytoplasm of the unstimulated cells. Of note, the increased fluorescence of Fluo-3 was detected in some cells, which was probably associated with spontaneous activation of the cells. Staining of RBL-2H3 cells with LysoTracker Red DND-99 revealed rather even distribution of secretory granules throughout the cytoplasm in the unstimulated cells. An increase in the level of calcium and a decrease in the number of granules in the cytosol were observed 2 min after the addition of A23187. Then, after just 7 min, the level of calcium in the cytosol elevated in many cells, while granules almost completely disappeared. Incubation of cells with 10 μ M UA caused similar, but less pronounced changes. Thus, similar to the calcium ionophore A23187, UA was able to induce intracellular Ca²⁺ elevation in RBL-2H3 cells.

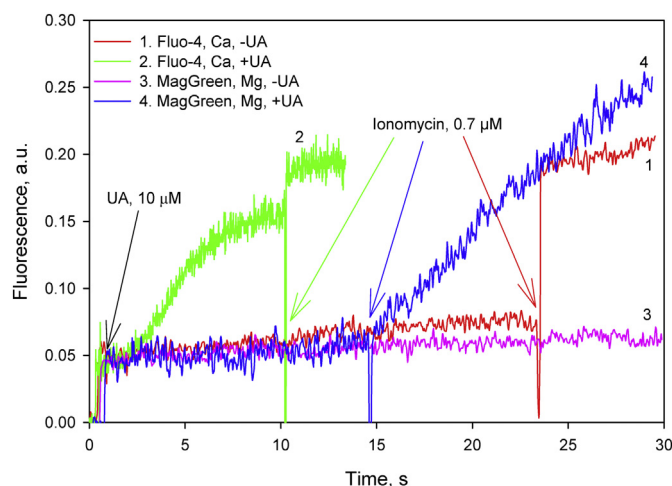


Fig. 4. Kinetics of calcium (curves 1, 2) or magnesium (curves 3, 4) influx into human red blood cells (RBC) measured by fluorescence of Fluo-4 or MagGreen. In addition to 10 mM CaCl₂ (curves 1,2) or 30 mM MgCl₂ (curves 3,4), the solution contained 150 mM NaCl, 10 mM Tris, 10 mM MES, pH = 7.4. Hematocrit was 1%. Ionomycin (0.7 μ M) was added at t = 10 min (2) or t = 15 min (4) to accelerate the influx of the cations. (For interpretation of the references to colour in this figure legend, the reader is referred to the web version of this article.)

3.5. Degranulation of RBL-2H3 cells

Based on the above data on the effect of UA on the intracellular calcium level and secretory granule dynamics, degranulation of the RBL-2H3 cells in the presence of UA could be expected. As seen in Fig. 6A (solid curve), the data on β -hexosaminidase release into the extracellular medium after 30-min incubation of the cells with UA in the concentration range of 0.2 to 10 μ M revealed a dose-dependent increase in RBL-2H3 cells degranulation starting from 1 μ M UA. The extent of the β -hexosaminidase release amounted to 25% at 10 μ M UA, which exceeded the level of spontaneous degranulation by 6.5-fold. For comparison, the level of RBL-2H3 cell degranulation induced by the calcium ionophore A23187 (1 μ M) was almost 45% (Fig. 6B). The concentration dependence of the A23187 effect on RBL-2H3 cell degranulation is shown in Fig. 6A (dotted curve). Pre-treatment of cells with 20 μ M BAPTA-AM (intracellular calcium chelator) led to a 2-fold

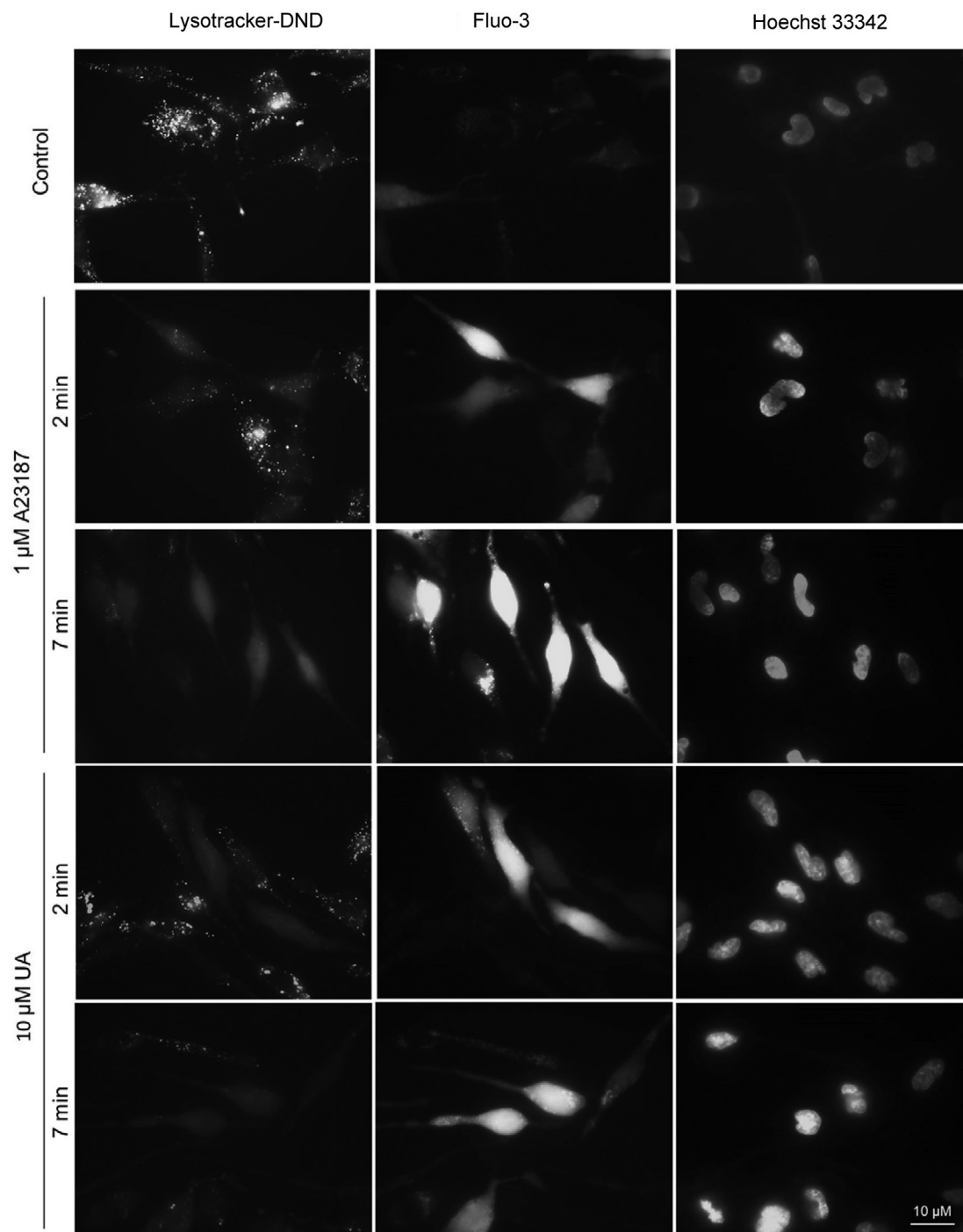


Fig. 5. Fluorescence microscopy of the secretory granules (labeled with LysoTracker Red DND-99) and the level of intracellular calcium (detected with Fluo-3) in RBL-2H3 cells. RBL-2H3 cells were stained with 5 μM Fluo-3-AM in the presence of 2.5 mM probenecid and 100 nM LysoTracker Red DND-99 for 30 min. After washing with HBSS, cells were stained with 2 μg/ml Hoechst 33342, stimulated with 1 μM A23187 or 10 μM UA and analyzed after 2 and 7 min. (For interpretation of the references to colour in this figure legend, the reader is referred to the web version of this article.)

and a 1.5-fold reduction in the degranulation induced by UA and A23187, respectively (Fig. 6B). Therefore, the UA-induced RBL-2H3 cell degranulation is apparently associated with changes in the intracellular Ca^{2+} level. Bearing in mind the ability of UA to cause mitochondrial uncoupling at low concentrations [3,27–29], we examined the effect of the classical protonophoric uncoupler carbonyl cyanide *m*-chlorophenylhydrazone (CCCP) on the degranulation level. As seen from Fig. 6A (dashed curve), incubation of RBL-2H3 cells with 10 μM CCCP caused only a slight release of β -hexosaminidase.

In summary, this paper comprises the data on the calcium-

transporting properties of UA in both artificial (liposomal) and natural (mitochondrial, erythrocyte and RBL-2H3 cell plasma) membranes. The Ca^{2+} ionophoric ability of UA is undoubtedly of high importance for its toxicity. It can be suggested that toxic side effects of UA on individuals using it as an antiobesity drug [1,2] might be due to a shift in calcium homeostasis. In addition, the Ca^{2+} -chelating propensity of UA might play a significant role in calcium accumulation by lichens and its toxicity for lichen photobionts [30–32].

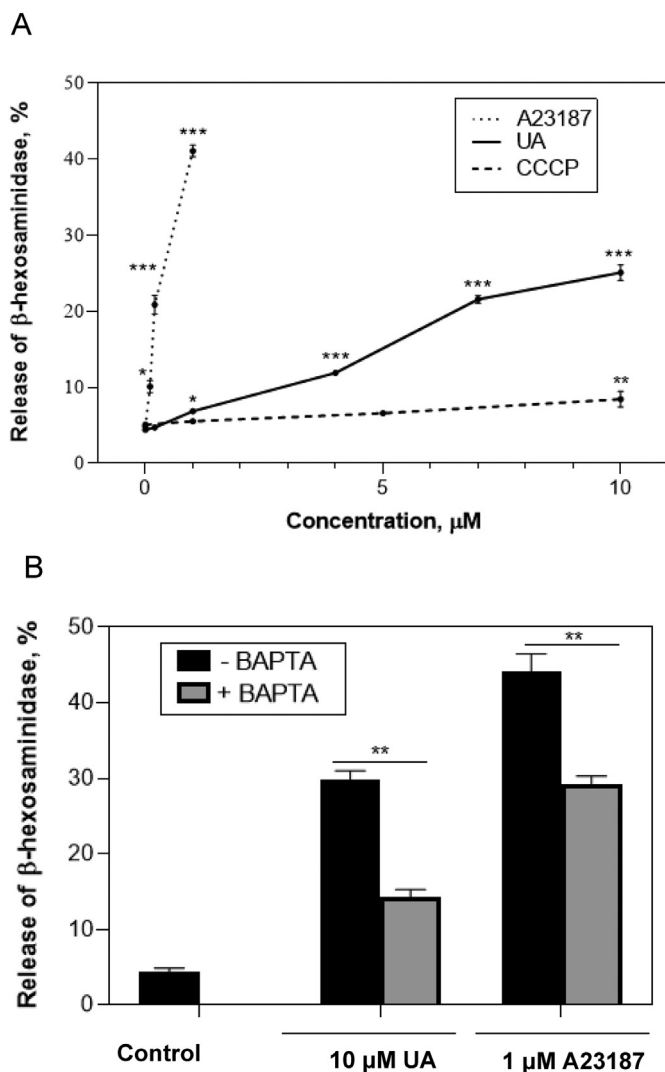


Fig. 6. Induction of RBL-2H3 cells degranulation with UA. **A.** Dose-dependent degranulation induced by UA (solid curve), by A23187 (dotted curve) or by the mitochondrial uncoupler CCCP (dashed curve). Results are expressed as mean \pm SEM ($n = 3$). Data were analyzed using one-way analysis of variance (ANOVA) with a Tukey post-hoc test. Statistical significance $*p \leq 0.05$, $**p \leq 0.01$, $***p \leq 0.001$ was calculated with respect to the unstimulated control cells. **B.** Pretreatment of the cells with the intracellular Ca^{2+} chelator BAPTA-AM (20 μM) for 30 min inhibited the degranulation induced by 10 μM UA or by 1 μM A23187. The level of β -hexosaminidase release (%), determined as the ratio of β -hexosaminidase activity in supernatants to the activity in cell lysates, was taken as a biomarker of degranulation. Results are expressed as mean \pm SEM ($n = 3$). $**p < 0.01$, Tukey post-hoc test.

Transparency document

The Transparency document associated this article can be found, in online version.

Acknowledgements

We are thankful to Leonid V. Belov and Arthur O. Zalevsky for technical assistance.

Funding

This work was financially supported by the Russian Science Foundation grant no. 16-14-10025 (studies of liposomes, isolated rat

liver mitochondria and erythrocytes) and by the joint RFBR and MOST research project no. 19-54-06003 (studies of RBL-2H3 cell degranulation).

References

- [1] L. Guo, Q. Shi, J.-L. Fang, N. Mei, A.A. Ali, S.M. Lewis, J.E.A. Leakey, V.H. Frankos, Review of usnic acid and usnea barbata toxicity, *Journal of Environmental Science and Health Part C* 26 (2008) 317–338.
- [2] A.A. Araujo, M.G. de Melo, T.K. Rabelo, P.S. Nunes, S.L. Santos, M.R. Serafini, M.R. Santos, L.J. Quintans-Junior, D.P. Gelain, Review of the biological properties and toxicity of usnic acid, *Nat.Prod.Res.* 29 (2015) 2167–2180.
- [3] Y.N. Antonenko, L.S. Khailova, T.I. Rokitskaya, E.S. Nosikova, P.A. Nazarov, O.A. Luzina, N.F. Salakhutdinov, E.A. Kotova, Mechanism of action of an old antibiotic revisited: role of calcium ions in protonophoric activity of usnic acid, *Biochim.Biophys.Acta Bioenerg.* 1860 (2019) 310–316.
- [4] J.C. Foreman, J.L. Mongar, B.D. Gomperts, Calcium ionophores and movement of histamine from isolated guinea pig mast cells stimulated by ionophore A23187 or by the anaphylactic reaction, *Naunyn Schmiedeberg's Arch. Pharmacol.* 302 (1978) 165–172.
- [5] F.L. Pearce, U. Blum, G. Poblete-Freundt, W. Schmutzler, Studies on the release of histamine from isolated guinea pig mast cells stimulated by ionophore A23187 or by the anaphylactic reaction, *Naunyn Schmiedeberg's Arch. Pharmacol.* 302 (1978) 165–172.
- [6] F.T. Crews, Y. Morita, A. McGivney, F. Hirata, R.P. Siraganian, J. Axelrod, IgE-mediated histamine release in rat basophilic leukemia cells: receptor activation, phospholipid methylation, Ca^{2+} flux, and release of arachidonic acid, *Arch.Biochem.Biophys.* 212 (1981) 561–571.
- [7] J.P. Bennett, S. Cockcroft, B.D. Gomperts, Ionomycin stimulates mast cell histamine secretion by forming a lipid-soluble calcium complex, *Nature* 282 (1979) 851–853.
- [8] A.I. Zebrev, Y.N. Antonenko, I.S. Gushchin, V.G. Voitenko, L.P. Ivanitskaya, T.P. Korobkova, M.K. Kudina, N.V. Murenets, T.A. Ivanova, T.N. Drobysheva, G.B. Ryazantsev, V.M. Fedoseev, Ionophore properties and histamine-releasing action of polyether antibiotic omomycin (985-I), *Biol.Membrany* 3 (1986) 1224–1231.
- [9] I.S. Gushchin, A.I. Zebrev, V.G. Voitenko, Histamine releasing action of calcium ionophore 985-I, *Agents and Actions* 23 (1988) 161–164.
- [10] N. Chakravarty, Calcium uptake in mast cells, energy metabolism and histamine secretion, *Agents and Actions* 20 (1987) 153–156.
- [11] T.C. Moon, A.D. Befus, M. Kulka, Mast cell mediators: their differential release and the secretory pathways involved, *Front.Immunol.* 5 (2014) 569.
- [12] E. Passante, N. Frankish, The RBL-2H3 cell line: its provenance and suitability as a model for the mast cell, *Inflamm. Res.* 58 (2009) 737–745.
- [13] F.H. Falcone, D. Wan, N. Barwary, RBL cells as models for in vitro studies of mast cells and basophils, *Immunol. Rev.* 282 (2018) 47–57.
- [14] L.M. Weatherly, A.J. Nelson, J. Shim, A.M. Rittano, E.D. Gerson, A.J. Hart, J. de Juan-Sanz, T.A. Ryan, R. Sher, S.T. Hess, J.A. Gosse, Antimicrobial agent triclosan disrupts mitochondrial structure, revealed by super-resolution microscopy, and inhibits mast cell signaling via calcium modulation, *Toxicol.Appl.Pharmacol.* 349 (2018) 39–54.
- [15] N. Fukuishi, S. Murakami, A. Ohno, N. Yamanaka, N. Matsui, K. Fukutsuji, S. Yamada, K. Itoh, M. Akagi, Does β -hexosaminidase function only as a degranulation indicator in mast cells? The primary role of β -hexosaminidase in mast cell granules, *J.Immunol.* 193 (2014) 1886–1894.
- [16] D. Johnson, H. Lardy, Isolation of liver or kidney mitochondria, *Methods Enzymol.* 10 (1967) 94–96.
- [17] K.E. Akerman, M.K. Wikstrom, Safranin as a probe of the mitochondrial membrane potential, *FEBS Lett.* 68 (1976) 191–197.
- [18] A.I. Sorochkina, S.I. Kovalchuk, E.O. Omarova, A.A. Sobko, E.A. Kotova, Y.N. Antonenko, Peptide-induced membrane leakage by lysine derivatives of gramicidin in liposomes, planar bilayers, and erythrocytes, *Biochim.Biophys.Acta* 1828 (2013) 2428–2435.
- [19] L. Yang, D.A. Andrews, P.S. Low, Lysophosphatidic acid opens a Ca^{++} channel in human erythrocytes, *Blood* 95 (2000) 2420–2425.
- [20] A. Sheshachalam, A. Baier, G. Eitzen, The effect of rho drugs on mast cell activation and degranulation, *J.Leukoc.Biol.* 102 (2017) 71–81.
- [21] W.L. Erdahl, C.J. Chapman, R.W. Taylor, D.R. Pfeiffer, Ionomycin, a carboxylic acid ionophore, transports Pb^{2+} with high selectivity, *J.Biol.Chem.* 275 (2000) 7071–7079.
- [22] M.V.Zamaraeva, A.I.Hagelgans, A.Y.Abramov, V.I.Ternovsky, P.G.Merzlyak, B.A. Tashmukhamedov, A.I.Saidkhodzhaev, Ionophoretic properties of ferutinin, *Cell Calcium* 22 (1997) 235–243.
- [23] A.Y. Abramov, M.V. Zamaraeva, A.I. Hagelgans, R.R. Azimov, O.V. Krasilnikov, Influence of plant terpenoids on the permeability of mitochondria and lipid bilayers, *Biochim.Biophys.Acta* 1512 (2001) 98–110.
- [24] P. Bernardi, V. Paradisi, T. Pozzan, G.F. Azzone, Pathway for uncoupler-induced calcium efflux in rat liver mitochondria: inhibition by ruthenium red, *Biochemistry* 23 (1984) 1645–1651.
- [25] L.B. Popova, E.S. Nosikova, E.A. Kotova, E.O. Tarasova, P.A. Nazarov, L.S. Khailova, O.P. Balezina, Y.N. Antonenko, Protonophoric action of triclosan causes calcium efflux from mitochondria, plasma membrane depolarization and bursts of miniature end-plate potentials, *Biochim.Biophys.Acta Biomembr.* 1860 (2018) 1000–1007.
- [26] L.B. Popova, A.L. Kamyshcheva, T.I. Rokitskaya, G.A. Korshunova, R.S. Kirsanov, E.A. Kotova, Y.N. Antonenko, Protonophoric and photodynamic effects of fluorescein decyl(triphenyl)phosphonium ester on the electrical activity of pond snail

- neurons, *Biochemistry (Mosc)* 84 (2019) 1151–1165.
- [27] R.B. Johnson, G. Feldott, H.A. Lardy, The mode of action of the antibiotic, usnic acid, *Arch.Biochem.* 28 (1950) 317–323.
- [28] A.N. Abo-Khatwa, A.A. Al-Robai, D.A. Al-Jawhari, Lichen acids as uncouplers of oxidative phosphorylation of mouse-liver mitochondria, *Nat.Toxins* 4 (1996) 96–102.
- [29] D. Han, K. Matsumaru, D. Rettori, N. Kaplowitz, Usnic acid-induced necrosis of cultured mouse hepatocytes: inhibition of mitochondrial function and oxidative stress, *Biochem.Pharmacol.* 67 (2004) 439–451.
- [30] M. Backor, J. Hudak, M. Repcak, W. Ziegler, M. Backorova, The influence of pH and lichen metabolites (vulpinic acid and (+) usnic acid) on the growth of the lichen photobiont *Trebouxia irregularis*, *Lichenologist* 30 (1998) 577–582.
- [31] M. Backor, S. Loppi, Interactions of lichens with heavy metals, *Biol. Plant.* 53 (2009) 214–222.
- [32] M. Backor, M. Backorova, M. Goga, M. Hrcka, Calcium toxicity and tolerance in lichens: Ca uptake and physiological responses, *Water Air and Soil Pollution* 228 (2017) 56.